



# Multielectrochromic amide-based poly(2,5-dithienylpyrrole) bearing a fluorene derivative: Synthesis, characterization, and optoelectronic properties

Jorge L. Neto<sup>a</sup>, Luis P.A. da Silva<sup>a</sup>, Joel B. da Silva<sup>a</sup>, Raul L. Ferreira<sup>b</sup>, Ana Júlia C. da Silva<sup>c</sup>, Júlio C.S. da Silva<sup>a</sup>, Ítalo N. de Oliveira<sup>b</sup>, Dimas J.P. Lima<sup>a</sup>, Adriana S. Ribeiro<sup>a,1,\*</sup>

<sup>a</sup> Chemistry and Biotechnology Institute, Federal University of Alagoas, Maceió, AL 57072-970, Brazil

<sup>b</sup> Physics Institute, Federal University of Alagoas, Maceió, AL 57072-970, Brazil

<sup>c</sup> Federal Institute of Alagoas, Campus Viçosa, Viçosa, AL 57700-000, Brazil



## ARTICLE INFO

### Article history:

Received 23 January 2021

Revised 11 March 2021

Accepted 13 March 2021

Available online 17 March 2021

### Keywords:

Synthesis

Conjugated polymer

Fluorescence

Spectroelectrochemistry

## ABSTRACT

A novel 2,5-dithienylpyrrole derivative bearing a fluorene substituent (SNSFCA) was synthesized and successfully electropolymerized on ITO electrodes in acetonitrile ( $\text{CH}_3\text{CN}$ ) containing tetrabutylammonium tetrafluoroborate ( $(\text{C}_4\text{H}_9)_4\text{NBF}_4$ ). The fluorescence properties of SNSFCA and its polymer (PSNSFCA) were investigated upon laser excitation at 337 nm, however, the polymer was not fluorescent, which may be explained by DFT methods. PSNSFCA films present multielectrochromism in a narrow range of applied potential ( $0.0 \leq E \leq 0.4$  V vs.  $\text{Ag}/\text{Ag}^+$ ), as shown by the track of the CIE 1931 xy chromaticity coordinates, besides high absorption in the near infrared (NIR) region. The electrochromic properties of PSNSFCA films, such as good chromatic contrast ( $\Delta T$ ), coloration efficiency ( $\eta$ ) in the range of  $110\text{--}350 \text{ cm}^2 \text{ C}^{-1}$ , and stability to redox cycling aroused the possibility of its application as an electrochromic material in optoelectronic devices.

© 2021 Elsevier Ltd. All rights reserved.

## 1. Introduction

The design and synthesis of novel  $\pi$ -conjugated polymers has attracted considerable interest due to their electrical and optical properties, leading to the development of multifunctional materials for technological applications in the field of electronics and photonics, sensors, and devices [1]. Polythiophene, polypyrrole and their derivatives have been highlighted as active layers in electrochromic device applications owing to their low band gap, good conductivity, high optical contrast, and multicolor electrochromism [2–4]. Furthermore, various strategies have been proposed in recent years to fine-tune the optical properties of these multifunctional materials, including the incorporation of fluorescent substituents [5,6], preparation of copolymers [7,8], and synthesis of fused-aromatic rings or extended  $\pi$ -conjugated systems [9].

Improved electrochromic properties than those of individual pyrrole and thiophene ones, may be achieved by using trimeric thiophene-pyrrole-thiophene derivatives, namely *N*-functionalized 2,5-dithienylpyrrole (SNS), which are synthesized from appropri-

ate pyrrole and thiophene coupling at their  $\alpha$ -positions [10]. The high reactivity of this  $\pi$ -extended system creates the possibility of introducing a series of functional groups through the nitrogen atom in the pyrrole ring of the SNS unit, such as alkyl and phenyl derivatives [11–14], ferrocene [15], BODIPY [16], luminol [17], dansyl [7], including a series of dyes [2,18] and fluorophores [19–21]. In addition, the relatively low oxidation potential (about 0.70 V vs.  $\text{Ag}/\text{Ag}^+$ ) [20], multielectrochromic properties, high chemical and electrochemical stability, and effortless synthesis methods, make PSNS derivatives one of the most promising conjugated polymers aimed at applications in optoelectronics [20,22].

According to Cihaner and Algi [21,23], the synthesis of extended  $\pi$ -conjugated systems based on the introduction of a fluorene appendage in the SNS main chain can render multifunctional materials that exhibit both electrochromic and fluorescent properties. Fluorene and polyfluorene derivatives have been widely employed in solar cells [24], sensors [25,26] and optical devices [27,28], due to their rigid planar structure, excellent hole-transporting properties, good solubility, exceptional chemical stability and photoluminescence efficiencies. Particularly, fluorene-9-carboxylic acid (FCAc), which contains an electron-withdrawing substituent, have rarely been studied [29], because its anodic oxidation is hampered

\* Corresponding author.

E-mail address: [aribeiro@qui.ufal.br](mailto:aribeiro@qui.ufal.br) (A.S. Ribeiro).

<sup>1</sup> ISE member

in common organic solvents, such as acetonitrile. However, the presence of a carboxyl group on the conjugated polymer backbone has several advantages owing to its electron-deficient functionality.

Therefore, the synthetic versatility of the SNS main chain along the aforementioned properties of fluorene-9-carboxylic acid moiety, has attracted a considerable interest in the synthesis of a novel SNS-fluorene derivative, namely N-(2-(2,5-di(thiophen-2-yl)-1H-pyrrol-1-yl)ethyl)-9H-fluorene-9-carboxamide (SNSFCA), for application as electrochromic material in optoelectronic devices.

## 2. Experimental

### 2.1. Materials and Instrumentation

All chemicals were purchased from Sigma-Aldrich or Acros as analytical grade. Previously to the synthetic procedures, the solvents  $\text{CH}_2\text{Cl}_2$  and toluene were treated with  $\text{P}_2\text{O}_5$ , being subsequently distilled. For the electrochemical experiments, anhydrous acetonitrile 99.8% ( $\text{CH}_3\text{CN} < 0.001\%$  water) and tetrabutylammonium tetrafluoroborate ( $(\text{C}_4\text{H}_9)_4\text{NBF}_4$ ) were used as received.

NMR spectra were recorded on a Bruker Ascend 600 spectrometer at 600 MHz for  $^1\text{H}$  NMR and 150 MHz for  $^{13}\text{C}$  NMR, using  $\text{CDCl}_3$  as solvent. Chemical shifts ( $\delta$ ) were given relative to tetramethylsilane (TMS) as the internal standard. The compounds were analyzed by using attenuated total reflection Fourier transformed infrared spectroscopy (ATR-FTIR) on a Shimadzu IR Prestige - 21 spectrophotometer, operating between  $4000 \text{ cm}^{-1}$  and  $400 \text{ cm}^{-1}$ , with a spectral resolution of  $4 \text{ cm}^{-1}$ . Scanning Electron Microscopy (SEM) images of the polymer film were obtained in a Jeol JSM - 6610 (Thermo Scientific NSS Spectral Image). A Hewlett-Packard 8453A diode array spectrophotometer was used for spectroelectrochemistry and kinetic studies.

### 2.2. Synthesis of N-(2-(2,5-di(thiophen-2-yl)-1H-pyrrol-1-yl)ethyl)-9H-fluorene-9-carboxamide (SNSFCA)

The starting materials 1,4-di(thiophen-2-yl)butane-1,4-dione and 2-(2,5-di(thiophen-2-yl)-1H-pyrrol-1-yl)ethanamine were synthesized according to the procedure previously described [7].

2-(2,5-di(thiophen-2-yl)-1H-pyrrol-1-yl)ethanamine (55 mg, 0.20 mmol), fluorene 9-carboxylic acid (FCAc) (84 mg, 0.40 mmol) and 4-dimethylaminopyridine (DMAP) (6.0 mg, 0.05 mmol) were added to  $\text{CH}_2\text{Cl}_2$  (5.0 mL) under stirring and argon atmosphere. The mixture was cooled with ice-salt bath ( $-2$  to  $0^\circ\text{C}$ ). Then a solution of N, N'-Dicyclohexylcarbodiimide (DCC) (41 mg, 0.20 mmol) in  $\text{CH}_2\text{Cl}_2$  (10 mL) was added dropwise. After this, the ice bath was removed, and the reaction mixture stirred for 20 h at room temperature. Dicyclohexylurea precipitated and was removed by filtration. The filtrate was extracted with  $\text{CH}_2\text{Cl}_2$  ( $5 \times 15$  mL) and  $\text{H}_2\text{O}$ , the organic solution was dried with anhydrous  $\text{Na}_2\text{SO}_4$  and the solvent was removed under reduced pressure. The crude product was purified by chromatography on silica gel using hexane/ethyl acetate 8:2 as eluent, to afford SNSFCA as grayish solid (65 mg, 73% yield), Scheme 1. **m.p.:**  $191 \pm 1^\circ\text{C}$ ;  **$^1\text{H}$  NMR (600 MHz,  $\text{CDCl}_3$ ,  $\delta$  (ppm)):** 7.8 (d,  $J = 7.56$  Hz, 2 H), 7.5 (dd,  $J = 0.72$ , 7.56 Hz, 2 H), 7.4 (t,  $J = 7.47$  Hz, 2 H), 7.3 (d,  $J = 1.08$ , 7.47 Hz, 2 H), 7.2 (d,  $J = 1.08$  Hz, 2 H), 7.0 (dd,  $J = 3.54$ , 5.16 Hz, 2 H), 6.9 (dd,  $J = 1.08$ , 3.54 Hz, 2 H), 6.3 (s, 2 H), 5.1 (s, 1 H), 4.7 (s, 1 H), 4.3 (t,  $J = 6.51$  Hz, 2 H), 3.2 (q,  $J = 6.34$  Hz, 2 H) (see Supplementary Material, Fig. S1);  **$^{13}\text{C}$  NMR (150 MHz,  $\text{CDCl}_3$ ,  $\delta$  (ppm)):** 172.0, 141.3, 141.1, 134.2, 128.6, 128.2, 127.7, 127.5, 126.2, 125.5, 125.4, 120.1, 111.4, 55.6, 43.8, 39.5 (see Supplementary Material, Fig. S2); **FTIR (ATR) ( $\text{cm}^{-1}$ )**: 3270 and 3100 ( $\nu_{\text{N}-\text{H}}$  amide), 3060 ( $\nu_{\text{C}-\text{H}}$  aromatic ring), 2960–2850 ( $\nu_{\text{sC}-\text{H}}$  and  $\nu_{\text{asC}-\text{H}}$ ), 1652 ( $\nu_{\text{C=O}}$  amide), 1608 ( $\nu_{\text{C=C}}$  aromatic ring), 1540 ( $\nu_{\text{C-N}}$  and  $\delta$

N-H amide), 1440 ( $\nu_{\text{C=C}}$  aromatic ring), 1210 ( $\nu_{\text{C-N}}$  amide), 1075 ( $\nu_{\text{C=C}}$  thiophene ring), 840 ( $\delta_{\text{C}-\text{H}_{\beta/\beta'}}$  thiophene ring), 730 ( $\delta_{\text{C}-\text{H}_{\beta}}$  pyrrole ring) and 678 ( $\delta_{\text{C}-\text{H}_{\alpha}}$  thiophene ring) (see Supplementary Material, Fig. S3).

### 2.3. Electropolymerization of SNSFCA

Films of PSNSFCA were electrodeposited on ITO electrodes (Delta Technologies, specific resistivity ( $R_s$ ) = 8–12  $\Omega \text{ cm}$ ,  $1.0 \text{ cm}^2$ ) in a single compartment cell. A home-built non-aqueous  $\text{Ag}/\text{Ag}^+$  (0.10 mol  $\text{L}^{-1}$   $\text{AgNO}_3/\text{CH}_3\text{CN}$ ), calibrated to the  $\text{Fc}/\text{Fc}^+$  redox system [30], was used as reference electrode and a Pt foil was employed as counter electrode. A solution of SNSFCA ( $5.0 \times 10^{-3}$  mol  $\text{L}^{-1}$ ) in 0.1 mol  $\text{L}^{-1}$   $(\text{C}_4\text{H}_9)_4\text{NBF}_4 / \text{CH}_3\text{CN}$  was used for the electrodeposition. The polymer was electrodeposited by cyclic voltammetry at scan rate ( $v$ ) = 20 mV  $\text{s}^{-1}$  in a potential range of  $0.00 \leq E \leq 0.65 \text{ V}$  vs.  $\text{Ag}/\text{Ag}^+$ . After electrodeposition, the films were washed several times with  $\text{CH}_3\text{CN}$  to remove unreacted monomers and the excess of electrolyte.

### 2.4. Spectroelectrochemistry

The PSNSFCA films deposited on ITO were characterized by cyclic spectrovoltammetry and double potential step spectrochronoamperometry in 0.1 mol  $\text{L}^{-1}$   $(\text{C}_4\text{H}_9)_4\text{NBF}_4 / \text{CH}_3\text{CN}$  solution as supporting electrolyte, using a Pt wire as the counter electrode and an  $\text{Ag}/\text{Ag}^+$  ( $\text{CH}_3\text{CN}$ ) electrode as reference. The cyclic voltammograms were registered in a potential range of  $-0.20 \leq E \leq 0.60 \text{ V}$  vs.  $\text{Ag}/\text{Ag}^+(\text{CH}_3\text{CN})$  at  $v = 20 \text{ mV s}^{-1}$  and chronoamperograms were acquired by applying pulses of  $E_1 = 0.00 \text{ V}$  and  $E_2 = 0.40 \text{ V}$  for 40 s. *In situ* spectroelectrochemistry was performed by recording the UV-vis-NIR spectra simultaneously with the electrochemical experiments in kinetic mode at intervals of 2.5 s.

The CIE (Commission Internationale de l'Eclairage) 1931 xy color coordinates [31] were calculated by using a Microsoft® Excel® spreadsheet developed by Mortimer and Varley [32,33] using a D55 standard illuminant. The CIE 1931 xy chromaticity coordinates in the CIE chromaticity diagram were displayed by the Spectra Lux Software v.2.0 Beta [34].

### 2.5. Fluorescence Spectroscopy

The photoluminescence emission spectra of SNSFCA solubilized in  $\text{CHCl}_3$  ( $0.5 \text{ mg mL}^{-1}$ ) and its polymer film deposited on ITO and in N-methylpyrrolidone (NMP) solution were recorded in an UV-Vis spectrometer (USB2000, Ocean Optics). The samples were excited by using a pulsed Nitrogen laser (MNL-103 PD LTB Lasertechnik Berlin) at 337 nm and pulse width of 3.0 ns. The repetition rate was set in 30 Hz.

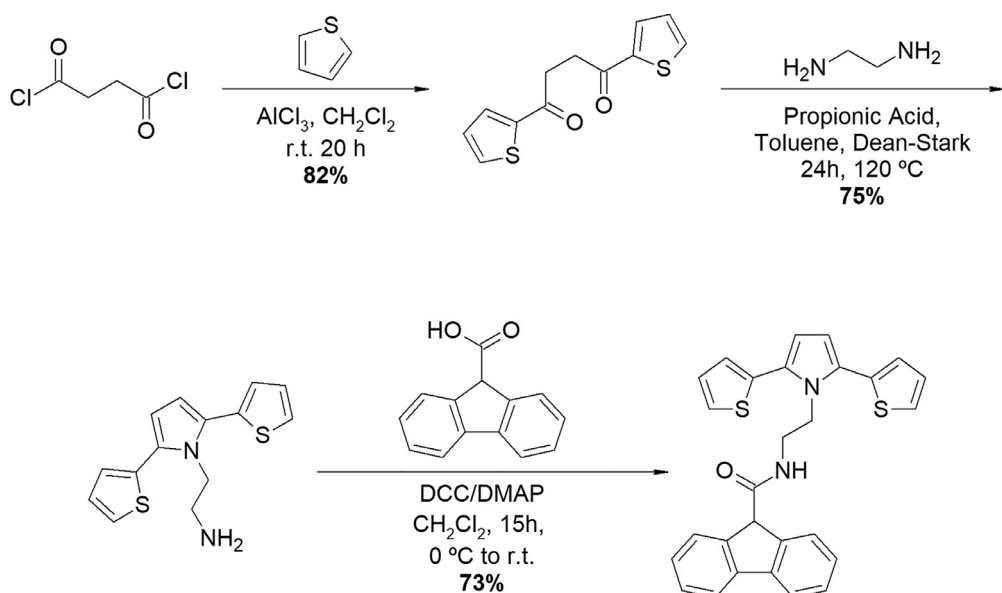
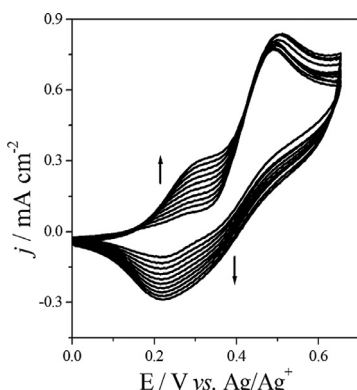
### 2.6. Computational methods

The quantum calculations were performed using the C.01 version of the Gaussian 09 program [35]. Ground state structures for SNSFCA and PSNSFCA were evaluated using the density functional theory (DFT) level of the three-parameter compound functional of Becke (B3LYP), including the D3 dispersion correction proposed by Grimme and co-workers [36]. All atoms of the monomer and its polymer were described using cc-pVDZ basis set [37].

## 3. Results and discussion

### 3.1. Synthesis and characterization of SNSFCA

The synthetic route to obtain SNSFCA was accomplished into three steps, as shown in Scheme 1. The first step involved the

**Scheme 1.** The synthetic route of SNSFCA.**Fig. 1.** Cyclic voltammograms of SNSFCA in  $0.1 \text{ mol L}^{-1}$   $(\text{C}_4\text{H}_9)_4\text{NBF}_4/\text{CH}_3\text{CN}$ .

preparation of the diketone involving a Friedel-Crafts acylation with 82% yield [12]. Then, a Paal-Knorr condensation between the diketone and ethylenediamine gave the SNS intermediate with 75% yield [38], and lastly, the condensation reaction between the FAc and the amine present in the SNS intermediate by using DCC/DMAP to afford SNSFCA as a greyish solid in 73% yield, **Scheme 1**. Such method has the simplicity, the use of mild conditions, and good yields from readily available starting materials as advantages.

### 3.2. Electropolymerization

The cyclic voltammograms recorded during the electropolymerization of SNSFCA show that the onset oxidation potential ( $E_{\text{onset}}$ ) of the monomer is *ca.* 0.60 V vs.  $\text{Ag}/\text{Ag}^+$  ( $\text{CH}_3\text{CN}$ ), which is lower than the oxidation potential reported for pyrrole (~ 0.90 V vs.  $\text{Ag}/\text{Ag}^+$  [39]), thiophene [40], and fluorenes [29,41,42]. When compared with most of SNS derivatives reported in the literature [21–23,42,43], the introduction of an electron donating fluorene amide-based substituent into the SNS main chain displaces the  $E_{\text{onset}}$  towards less anodic potentials [44], facilitating the electropolymerization process. Furthermore, from cyclic voltammograms shown in **Fig. 1**, a new redox pair in the range of  $0.10 \leq E \leq 0.40$  V vs.  $\text{Ag}/\text{Ag}^+$  arised. It was observed that the current density increases

with the repetitive cyclic voltammetric scans, which implies that the deposition of a redox-active layer of a conducting material is occurring on the electrode.

### 3.3. Morphological characterization

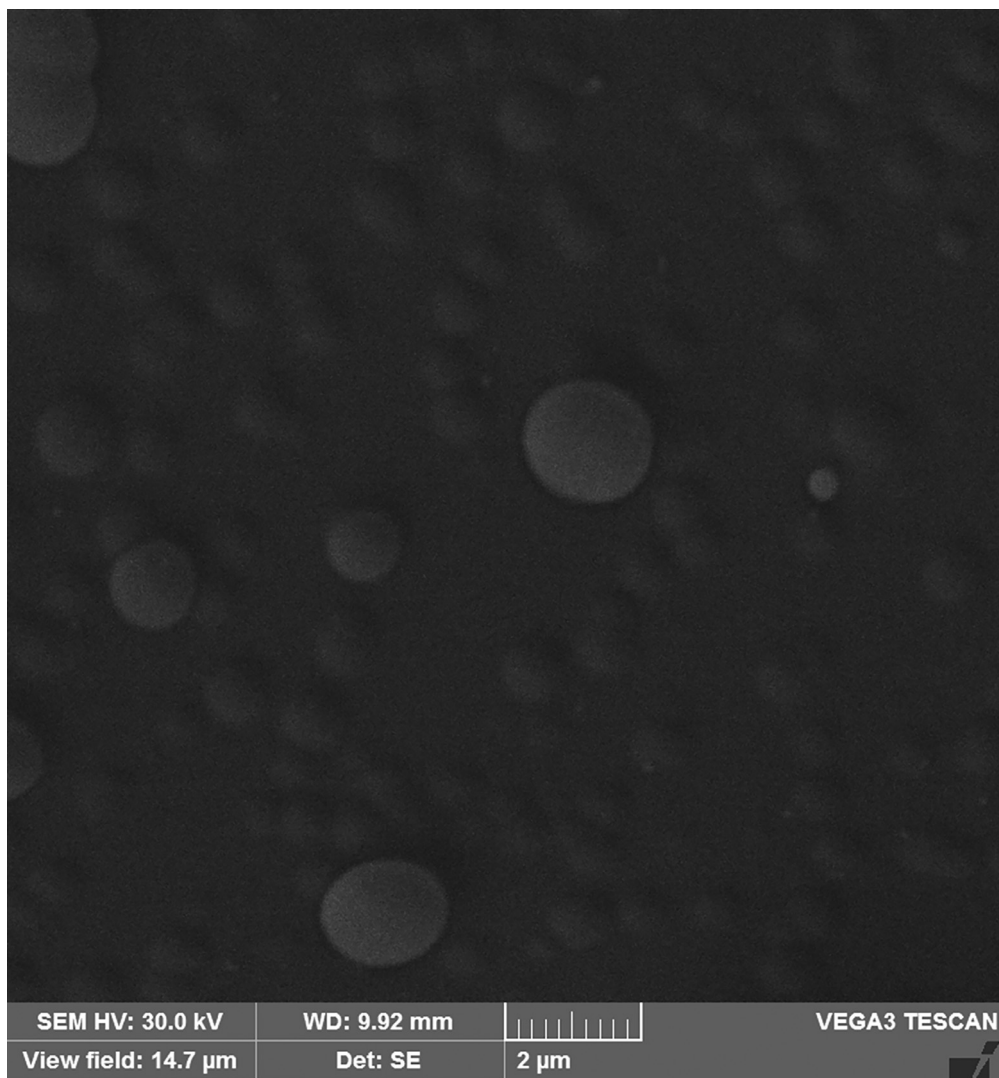
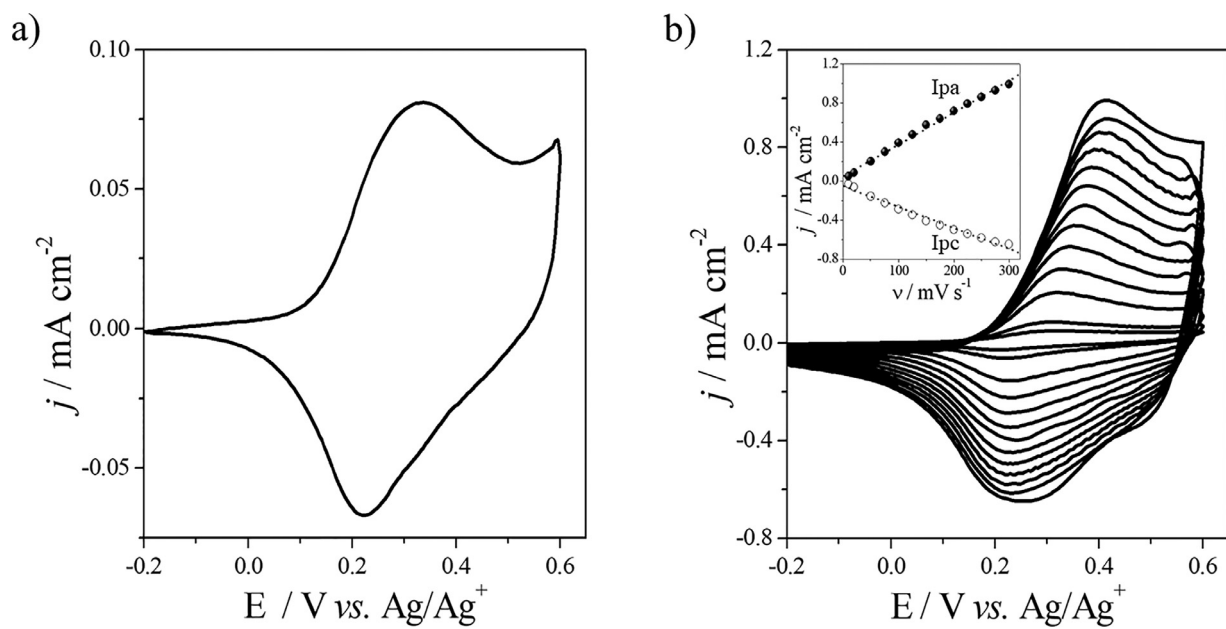
The SEM image of the PSNSFCA film deposited on ITO displays a smooth, homogenous and globular morphology. The potentiodynamic method (cyclic voltammetry) used for the electrodeposition of the polymer on ITO usually results in multi-nucleation leading to small, but well-dispersed, grains [45], as can be seen in **Fig. 2**. Such structures are similar to those found for other poly(2,5-dithienylpyrrole) derivatives reported in the literature [46].

### 3.4. Spectroelectrochemical characterization

The cyclic voltammogram of the PSNSFCA film deposited on ITO (**Fig. 3a**) displayed an anodic wave with anodic peak potential ( $E_{\text{pa}}$ ) at 0.33 V and a cathodic wave with cathodic peak potential ( $E_{\text{pc}}$ ) at 0.22 V vs.  $\text{Ag}/\text{Ag}^+$ . The difference ( $\Delta E_{\text{p}}$ ) of 0.11 V between the  $E_{\text{pa}}$  and  $E_{\text{pc}}$  is within the range of commonly observed values for conjugated polymers and have been associated to the kinetic limitations, such as slow heterogeneous electron transfer, effects of structural reorganization processes within the polymer film, and electronic charging of a sum of two interfacial exchanges, namely the electrode/polymer and the polymer solution interfaces [47,48].

The polymer film was cycled between reduced, neutral and oxidized states at various scan rates, in order to investigate the scan rate dependence of anodic ( $I_{\text{pa}}$ ) and cathodic ( $I_{\text{pc}}$ ) peak currents. The peak currents were linearly proportional to the scan rate indicating a non-diffusional redox process and a well-adhered electroactive polymer films to the working electrode surface [49], **Fig. 3b**.

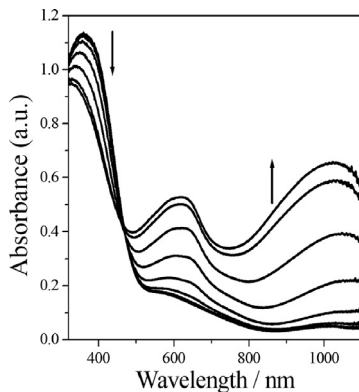
The changes in the absorbance spectra of the PSNSFCA film according to the applied potential are shown in **Fig. 4**. In this case, a potential range of 0.00 V to 0.40 V was sufficient to cause a perceptible optical contrast in a reversible way. At 0.00 V (neutral state), the absorption spectrum of the polymer film exhibited a band with maximum wavelength ( $\lambda_{\text{max}}$ ) at 360 nm, assigned to  $\pi-\pi^*$  transition. The band gap energy ( $E_{\text{g}}$ ) of 2.40 eV was calculated from the onset of the  $\pi-\pi^*$  transition ( $\lambda_{\text{onset}} = 517$  nm) in the absorption spectrum of the film at neutral state. According to

**Fig. 2.** SEM image of PSNSFCA film electrodeposited on ITO.**Fig. 3.** Cyclic voltammograms of the PSNSFCA film deposited on ITO in  $0.1 \text{ mol L}^{-1} (\text{C}_4\text{H}_9)_4\text{NBF}_4/\text{CH}_3\text{CN}$ , (a) at  $v = 0.02 \text{ V s}^{-1}$  and (b) at different scan rates between  $0.025$  and  $0.300 \text{ V s}^{-1}$ . The inset shows a plot of the peak current density on the potential sweep rate.

**Table 1**

Optical properties of PFCAc and PSNS-fluorene derivatives.

Polymer	$\lambda_{\text{max}}$ (nm)	$E_g$ (eV)	Colors	Ref.
	374	3.10	transparent (0.00 V), brownish-orange (1.25 V) <sup>a</sup>	[42]
	445	2.18	yellow (0.00 V), green/blue (intermediate), violet (0.80 V) <sup>b</sup>	[21,23]
	323	2.59	yellow (0.00 V), blue (1.00 V) <sup>c</sup>	[52]
	360	2.40	yellow (0.00 V), green (intermediate), blue (0.40 V) <sup>c</sup>	This work

<sup>a</sup> E (V) vs. Ag wire,<sup>b</sup> E (V) vs. Ag/AgCl,<sup>c</sup> E (V) vs. Ag/Ag<sup>+</sup>. The conversion factors for the reference electrodes are + 0.10 V relative to pseudo reference Ag wire [53] and -0.20 V relative to Ag/AgCl [54,55].**Fig. 4.** Spectroelectrochemistry of PSNSFCA film deposited on ITO in 0.1 mol L<sup>-1</sup> (C<sub>4</sub>H<sub>9</sub>)<sub>4</sub>NBF<sub>4</sub> / CH<sub>3</sub>CN. Spectra were registered at each 50 mV from 0.00 to 0.40 V vs. Ag/Ag<sup>+</sup> (CH<sub>3</sub>CN).

the literature,  $E_g$  values for conjugated polymers are in the range of 1.5–3.0 eV [9,50,51]. Therefore, the  $E_g$  value found for PSNSFCA films is close to the values reported for similar  $\pi$ -conjugated systems, including other PSNS-fluorene derivatives [21,23,52], and it is lower than that exhibited by PFCAc [42], as can be seen in Table 1.

With increasing potential, the peak intensity of the band at 360 nm slightly decreased, and an isosbestic point may be ob-

served at 470 nm indicating that polymer film is undergoing interconversion between its neutral and oxidized states. At higher oxidation levels, two broad bands at ca. 620 and 1030 nm appeared, owing to the formation of polaronic and bipolaronic states, respectively [56,57].

It is well known that the absorption spectrum of an electrochromic film provides an objective measure for color absorption in visible region. However, such measurement is limited in terms of how the color is perceived by the human eye. To overcome this drawback, the field of colorimetry has been developed for description of color in an objective way [32]. Hence, *in-situ* colorimetric analysis were performed for quantitative examination of PSNSFCA spectral properties, thus providing a direct correlation between the changes in the spectral absorption bands as the colors seen by the human eye according to the potential applied to the system. The CIE 1931 xy chromaticity coordinates were calculated from the *in situ* spectra of the polymer film at potentials varying from 0.00 to 0.40 V and its trajectory is shown in Fig. 5, together with the images of the film in different oxidation states. The colors of the film change from yellow ( $x = 0.388$ ,  $y = 0.425$ ) in the neutral state (0.00 V), green ( $x = 0.336$ ,  $y = 0.382$ ) in the intermediate state, to blue ( $x = 0.317$ ,  $y = 0.354$ ) in the oxidized state.

It is noteworthy the PSNSFCA film presents multielectrochromism where a gradual change in the chromatic coordinates takes place as the potential is varied in a narrow range of 0.40 V. Such a high electrochromic response of PSNSFCA film contrasts

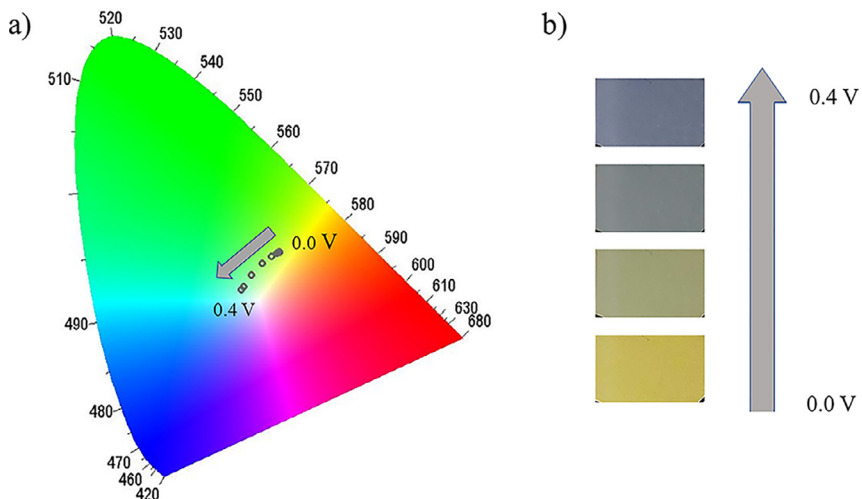


**Fig. 5.** (a) Calculated colour trajectory in the CIE 1931 xy color space and (b) images of the PSNSFCA film deposited on ITO, registered during potential scan from 0.00 to 0.40 V vs. Ag/Ag<sup>+</sup> (CH<sub>3</sub>CN) (For interpretation of the references to color in this figure, the reader is referred to the web version of this article.).

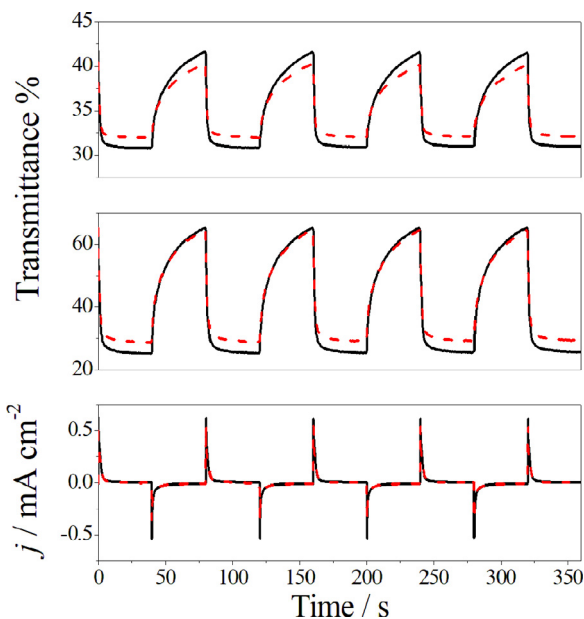


**Fig. 6.** Transmittance variation at (a)  $\lambda = 620$  nm and (b)  $1030$  nm, and (c) current density ( $j$ ) variation for the PSNSFCA film during double potential step chronoamperometry with  $E_1 = 0.0$  V,  $E_2 = 0.4$  V and  $t_{\text{step}} = 40$  s. Full line (black) corresponds to the first cycle and dashed line (red) corresponds to the 100th cycle (For interpretation of the references to color in this figure legend, the reader is referred to the web version of this article.).

with the typical behavior of similar SNS-based polymers, in which the potential range for a significant electrochromic response may reaches up to 3.0 V [58]. Thus, these features make it suitable for application as active layer in displays and electrochromic devices.

### 3.5. Electrochromic properties

The electrochromic performance of the PSNSFCA film with respect to chromatic contrast ( $\Delta\%T$ ), coloration efficiency ( $\eta$ ) and stability to redox cycling was investigated by double step spectrochronoamperometry. The variation in the transmittance (%) of the polymer film recorded simultaneously at 620 and 1030 nm in function of the number of redox cycles is depicted in Fig. 6 and the  $\Delta\%T$  calculated at such wavelengths were 11.8% and 41.3%, respec-

tively, indicating that the polymer films present pronounced chromatic contrast in the NIR region. This characteristic is an advantage due to the possibility of application of this polymer in smart windows that controls the temperature of the ambient by absorbing NIR radiation.

The coloration efficiency ( $\eta$ ) was calculated from the amount of the charge injected in the polymer as a function of the change in the optical density during switching. The  $\eta$  values calculated for the PSNSFCA film at 620 and 1030 nm were  $110$  and  $350 \text{ cm}^2 \text{ C}^{-1}$ , respectively. These values are higher than those cited in the literature for PSNS-fluorene derivatives ( $78 - 107 \text{ cm}^2 \text{ C}^{-1}$ ) [21,23,52]. Therefore, concerning energy economy, PSNSFCA is a promising material for application in electrochromic devices, because it needs only a small amount of charge injected per area to show a perceptible change of its color.

The PSNSFCA film is stable with respect to the switch between the oxidized and reduced states by over than 100 cycles, showing no significant loss of its electrical and optical responses, Fig. 6. Coulombic efficiency was calculated as being 91% in the initial cycles, reaching 94% in subsequent cycles, such behavior may be attributed to the conformational changes in the structure of the film that occurs during the redox process [59].

### 3.6. Fluorescence properties

The fluorescence properties of polyfluorene and its derivatives are well-known and broadly reported in the literature as having a strong blue emission about between 400 and 500 nm [21,28,29,60]. Therefore, it would expected that both monomer and polymer derivatized with a fluorene moiety were fluorescent. Indeed, the monomer presents a blue emission, which is characterized by a dual fluorescence with bands centered at 424 and 526 nm, indicating that distinct radiative mechanisms in SNSFCA photoluminescence occur. For organic compounds, this behavior is usually attributed to the excited states associated with distinct molecular conformations [61], excimer formation [62,63], and photodimerization [62,64].

Interestingly, it was observed a pronounced color change in the SNSFCA solution from colorless to brownish after the laser excitation. In order to investigate such behavior, the modification in the emission spectrum of SNSFCA in different time intervals after the initial UV excitation was analyzed, Fig. 7a. After the initial UV excitation, a modification in the SNSFCA fluorescence takes place with

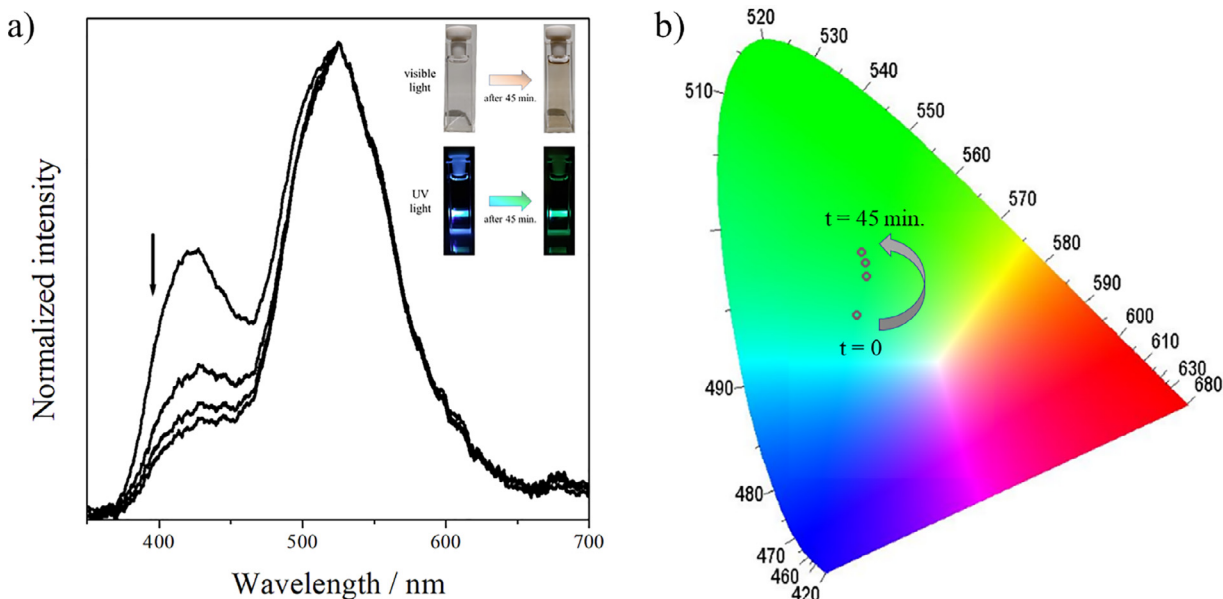


**Fig. 7.** (a) Normalized fluorescence spectra of SNSFCA according to the time after UV laser exposure from  $t = 0$ , 5 min, 25 min and 45 min. Inset: images of SNSFCA before ( $t = 0$ ) and after UV laser exposure (45 min.) under visible and UV light. (b) Calculated colour trajectory (emission) in the CIE 1931 xy color space before ( $t = 0$ ) and after UV laser exposure at 5, 25 and 45 min.

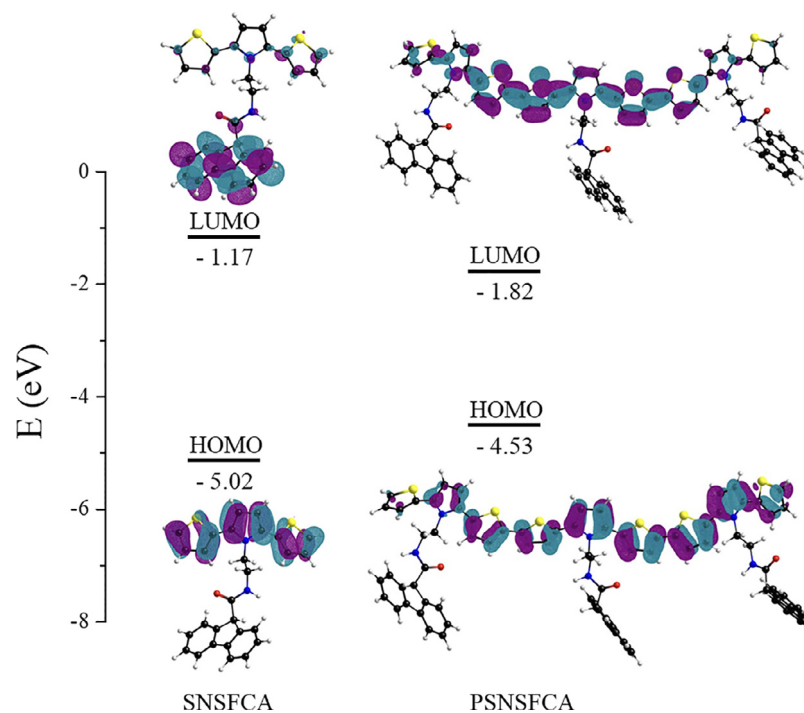


**Fig. 8.** The HOMO and LUMO Kohn-Sham molecular orbitals of the SNSFCA and PSNSFCA.

a strong suppression of the fluorescence band centered at 424 nm. In this case, the exposure of SNSFCA solution to UV laser for a long period of time leads to an irreversible change of its optical properties due to photodimerization [62,64].

Although the fluorescence emission of SNSFCA solution is maintained after the formation of stable dimers, the photoluminescence of PSNSFCA film and solution was not observed. In such a case, the SNS polymer chain seems to suppress the radiative decaying of excited electrons, as discussed by the analysis of HOMO and LUMO theoretical calculations of the monomer and polymer structures.

### 3.7. Computational Results

According to Fig. 8, the HOMO orbital for SNSFCA is distributed along the conjugated rings of thiophene and pyrrole of the SNS system, while the LUMO orbitals are strictly located in the fluorene group. However, the polymerization drastically affects the LUMO orbital of the molecular structure of the compound, in which for the PSNSFCA, both HOMO and LUMO orbitals are symmetrically distributed in the conjugated region of the SNS aromatic rings. This result is consistent with the fluorescence behavior of the material,

since it is possible to observe that the monomer is a blue/green light emitter, whilst the polymer is not fluorescent.

Moreover, the band gap energy of the SNSFCA and PSNSFCA were calculated using the HOMO-LUMO difference as being 3.85 eV and 2.71 eV, respectively. Such result is in good agreement with the PSNSFCA  $E_g^{op}$  of 2.40 eV.

#### 4. Conclusions

The monomer SNSFCA was prepared by using a simple synthetic route with good yield (73%) and its electropolymerization on ITO was successfully achieved. PSNSF films exhibited multielectrochromic behavior, presenting distinct colors from yellow in the neutral state, green in the intermediate state, to blue in the oxidized state. It would be expected that both monomer and polymer derivatized with a fluorene moiety were fluorescent, however, the monomer presents a blue emission, whilst the photoluminescence of the polymer was not observed. Such behavior was interpreted theoretical calculations in good agreement with the results.

The electrochromic properties showed by the PSNSFCA films, such as good chromatic contrast ( $\Delta\%T$ ), coloration efficiency ( $\eta$ ) and stability to switching, including high absorption in the NIR region ( $\Delta\%T$  at 1030 nm = 41.3%), aroused the interest in the application of this polymer as active layer in electrochromic devices and displays.

#### Declaration of Competing Interest

The authors declare that they have no known competing financial interests or personal relationships that could have appeared to influence the work reported in this paper.

#### Credit authorship contribution statement

**Jorge L. Neto:** Methodology, Formal analysis, Investigation, Validation, Writing – original draft. **Luis P.A. da Silva:** Investigation, Validation. **Joel B. da Silva:** Investigation, Validation. **Raul L. Ferreira:** Investigation, Validation. **Ana Júlia C. da Silva:** Methodology, Formal analysis, Investigation, Supervision. **Júlio C.S. da Silva:** Formal analysis, Writing – original draft. **Ítalo N. de Oliveira:** Formal analysis, Investigation, Writing – original draft. **Dimas J.P. Lima:** Conceptualization, Formal analysis, Resources, Writing – original draft, Supervision, Funding acquisition. **Adriana S. Ribeiro:** Conceptualization, Formal analysis, Resources, Writing – review & editing, Project administration, Funding acquisition.

#### Acknowledgments

The authors wish to thank the granting authorities CNPq (proc. 442320/2014-0), CAPES and FAPEAL (proc. 1033/2016 and 60030 393/2017) for financial support. Also wish thank to Prof. J.D. de Freitas at Federal Institute of Alagoas for the SEM image.

#### Supplementary materials

Supplementary material associated with this article can be found, in the online version, at [doi:10.1016/j.electacta.2021.138173](https://doi.org/10.1016/j.electacta.2021.138173).

#### References

- [1] M.P. Algi, A. Cihaner, F. Algi, Design, synthesis, photochromism and electrochemistry of a novel material with pendant photochromic units, *Tetrahedron* 70 (2014) 5064–5072.
- [2] D. Yiğit, Ş.O. Hacıoğlu, M. Güllü, L. Toppare, Novel poly(2,5-dithienylpyrrole) (PSNS) derivatives functionalized with azobenzene, coumarin and fluorescein chromophore units: Spectroelectrochemical properties and electrochromic device applications, *New J. Chem.* 39 (2015) 3371–3379.
- [3] K.H. Chang, H.P. Wang, T.Y. Wu, J.W. Sun, Optical and electrochromic characterizations of four 2,5-dithienylpyrrole-based conducting polymer films, *Electrochim. Acta* 119 (2014) 225–235.
- [4] T.Y. Wu, J.W. Liao, C.Y. Chen, Electrochemical synthesis, characterization and electrochromic properties of indan and 1,3-benzodioxole-based poly(2,5-dithienylpyrrole) derivatives, *Electrochim. Acta* 150 (2014) 245–262.
- [5] W.M. Pazin, A.K.A. Almeida, V. Manzoni, J.M.M. Dias, A.C.F. de Abreu, M. Navarro, A.S. Ito, A.S. Ribeiro, I.N. de Oliveira, Thermal and solvatochromic effects on the emission properties of dansyl-based thiophene derivative, *RSC Adv.* 10 (2020) 28484.
- [6] R. Ayrancı, M. Ak, A fluorescence and electroactive surface design electropolymerization of dansyl fluorophore functionalized PEDOT, *J. Electrochem. Soc.* 164 (2017) H925–H930.
- [7] J.L. Neto, L.P.A. da Silva, J.B. da Silva, A.J.C. da Silva, D.J.P. Lima, A.S. Ribeiro, A rainbow multielectrochromic copolymer based on 2,5-di(thienyl)pyrrole derivative bearing a dansyl substituent and 3,4-ethylenedioxythiophene, *Synth. Met.* 269 (2020) 116545.
- [8] A.J.C. Silva, V.C. Nogueira, T.E.A. Santos, C.J.T. Buck, D.R. Worrall, J. Tonholo, R.J. Mortimer, A.S. Ribeiro, Copolymerisation as a way to enhance the electrochromic properties of an alkylthiophene oligomer and a pyrrole derivative: copolymer of 3,3''' dihexyl-2,2':5',2":5",2'''-quaterthiophene with (R)-(-)-3-(1-pyrrolyl)propyl-N-(3,5-dinitrobenzoyl)- $\alpha$ -phenylglycinate, *Sol. Energy Mater. Sol. Cells* 134 (2015) 122–132.
- [9] A.S. Ribeiro, R.J. Mortimer, Conjugated conducting polymers with electrochromic and fluorescent properties, in: *SPR Electrochemistry*, v. 13, 1st ed., Cambridge, UK, 2016, pp. 21–49.
- [10] E. Rende, C.E. Kılıç, Y.A. Uđum, D. Toffoli, L. Toppare, Electrochromic properties of multicolored novel polymer synthesized via combination of benzotriazole and N-functionalized 2,5-di(2-thienyl)-1H-pyrrole units, *Electrochim. Acta* 138 (2014) 454–463.
- [11] P. Camurlu, C. Gültekin, Z. Bicil, Fast switching, high contrast multichromic polymers from alkyl-derivatized dithienylpyrrole and 3,4-ethylenedioxythiophene, *Electrochim. Acta* 61 (2012) 50–56.
- [12] S. Tarkuc, M. Alk, E. Onurhan, L. Toppare, Electrochromic properties of "trimeric" thiophene-pyrrole-thiophene derivative grown from electrodeposited 6-(2,5-di-thiophen-2-yl-1H-pyrrolyl-1-yl)hexan-1-amine and its copolymer, *J. Macromol Sci. Part A Pure Appl. Chem.* 45 (2008) 164–171.
- [13] N.A. Lengkeek, J.M. Harrowfield, G.A. Koutsantonis, Synthesis and electropolymerization of N-(4'-carboxyphenyl)-2,5-di(2"-thienyl)pyrrole, *Synth. Met.* 160 (2010) 72–75.
- [14] E. Yıldız, P. Camurlu, C. Tanyeli, I. Akhmedov, L. Toppare, A soluble conducting polymer of 4-(2,5-di(thiophene-2-yl)-1H-pyrrol-1-yl)benzamine and its multichromic copolymer with EDOT, *J. Electroanal. Chem.* 612 (2008) 247–256.
- [15] P. Camurlu, Z. Bicil, C. Gültekin, N. Karagoren, Novel ferrocene derivatized poly(2,5-dithienylpyrroles): optoelectronic properties, electrochemical copolymerization, *Electrochim. Acta* 63 (2012) 245–250.
- [16] A. Cihaner, F. Algi, A new conducting polymer bearing 4,4-difluoro-4-bora-3a,4a-diaza-s-indacene (BODIPY) subunit: synthesis and characterization, *Electrochim. Acta* 54 (2008) 786–792.
- [17] D. Asil, A. Cihaner, F. Algi, A.M. Önal, A diverse-stimuli responsive chemiluminescent probe with luminol scaffold and its electropolymerization, *Electroanalysis* 22 (2010) 2254–2260.
- [18] A. Cihaner, F. Algi, Electrochemical and optical properties of new soluble dithienylpyrroles based on azo dyes, *Electrochim. Acta* 54 (2009) 1702–1709.
- [19] B. Hu, C. Li, Z. Liu, X. Zhang, W. Luo, L. Jin, Synthesis and multi-electrochromic properties of asymmetric structure polymers based on carbazole-EDOT and 2,5-dithienylpyrrole derivatives, *Electrochim. Acta* 305 (2019) 1–10.
- [20] S. Koyuncu, C. Zafer, E. Sefer, F.B. Koyuncu, S. Demic, I. Kaya, E. Ozdemir, S. Icli, A new conducting polymer of 2,5-bis(2-thienyl)-1H-(pyrrole) (SNS) containing carbazole subunit: electrochemical, optical and electrochromic properties, *Synth. Met.* 159 (2009) 2013–2021.
- [21] A. Cihaner, F. Algi, Processable electrochromic and fluorescent polymers based on N-substituted thiénylpyrrole, *Electrochim. Acta* 54 (2008) 665–670.
- [22] W.H. Wang, J.C. Chang, T.Y. Wu, 4-(Furan-2-yl)phenyl-containing polydithienylpyrroles as promising electrodes for high contrast and coloration efficiency electrochromic devices, *Org. Electron.* 74 (2019) 23–32.
- [23] A. Cihaner, F. Algi, A processable rainbow mimic fluorescent polymer and its unprecedented coloration efficiency in electrochromic device, *Electrochim. Acta* 53 (2008) 2574–2578.
- [24] J. Hu, J. You, C. Peng, S. Qiu, W. He, C. Li, X. Liu, Y. Mai, F. Guo, Polyfluorene copolymers as high-performance hole-transport materials for inverted Perovskite solar cells, *RRL Sol.* 4 (2020) 1900384.
- [25] Q. Hu, W. Zhang, Q. Yin, Y. Wang, H. Wang, A conjugated fluorescent polymer sensor with amidoxime and polyfluorene entities for effective detection of uranyl ion in real samples, *Spectrochim. Acta Part A Mol. Biomol. Spectrosc.* 244 (2021) 118864.
- [26] S. Roy, A. Gunukula, B. Ghosh, C. Chakraborty, A folic acid-sensitive polyfluorene based "turn-off" fluorescence nanoprobe for folate receptor overexpressed cancer cell imaging, *Sens. Actuators B Chem.* 291 (2019) 337–344.
- [27] F.A.R. Nogueira, A.J.C. Silva, J.D. Freitas, A.S. Tintino, A.P.L.A. Santos, I.N. Oliveira, A.S. Ribeiro, Transmissive to dark electrochromic and fluorescent device based on poly(fluorene-bisthiophene) derivative, *J. Braz. Chem. Soc. Spec. Issue Braz. Woman Sci.* 30 (12) (2019) 2702–2711.
- [28] S.P. Mucur, C. Kök, H. Bilgili, B. Canimkurbey, S. Koyuncu, Conventional and inverted organic light emitting diodes based on bright green emissive polyfluorene derivatives, *Polymer* 151 (2018) 101–107.

- [29] G. Nie, T. Cai, J. Xu, S. Zhang, Low-potential facile electrosyntheses of high-quality free-standing poly(fluorene-9-carboxylic acid) films, *Electrochim. Commun.* 10 (2008) 186–189.
- [30] G. Gritzner, J. Kuta, Recommendations on reporting electrode potentials in nonaqueous solvents, *Pure Appl. Chem.* 56 (1984) 461–466.
- [31] G. Wyszecki, W.S. Stiles, *Color Science: Concepts and Methods, Quantitative Data and Formulae*, 2nd ed., John Wiley Ans Sons, New York, USA, 1982.
- [32] R.J. Mortimer, T.S. Varley, Quantification of colour stimuli through the calculation of CIE chromaticity coordinates and luminance data for application to *in situ* colorimetry studies of electrochromic materials, *Displays* 32 (2011) 35–44.
- [33] R.J. Mortimer, T.S. Varley, *In situ* spectroelectrochemistry and colour measurement of a complementary electrochromic device based on surface-confined prussian blue and aqueous solution-phase methylviologen, *Sol. Energy Mater. Sol. Cells* 99 (2012) 213–220.
- [34] P.A. Santa-Cruz, F.S. Teles, Spectra Lux Software v. 2.0 Beta, Ponto Quântico Nanodispositivos/RENAMI, Brasil, 2003.
- [35] M.J. Frisch, G.W. Trucks, H.B. Schlegel, G.E. Scuseria, M.A. Robb, J.R. Cheeseman, G. Scalmani, V. Barone, B. Mennucci, G.A. Petersson, H. Nakatsuji, M. Caricato, X. Li, H.P. Hratchian, A.F. Izmaylov, J. Bloino, G. Zheng, J.L. Sonnenberg, M. Hada, M. Ehara, K. Toyota, R. Fukuda, J. Hasegawa, M. Ishida, T. Nakajima, Y. Honda, O. Kitao, H. Nakai, T. Vreven, J.A. Montgomery Jr., J.E. Peralta, F. Ogliaro, M. Bearpark, J.J. Heyd, E. Brothers, K.N. Kudin, V.N. Staroverov, R. Kobayashi, J. Normand, K. Ragahavachari, A. Rendell, J.C. Burant, S.S. Iyengar, J. Tomasi, M. Cossi, N. Rega, J.M. Millam, M. Klene, J.E. Knox, J.B. Cross, V. Bakken, C. Adamo, J. Jaramillo, R. Gomperts, R.E. Stratmann, O. Yazyev, A.J. Austin, R. Cammi, C. Pomelli, J.W. Ochterski, R.L. Martin, K. Morokuma, V.G. Zakrzewski, G.A. Voth, P. Salvador, J.J. Dannenberg, S. Dapprich, A.D. Daniels, Ö. Farkas, J.B. Foresman, J.V. Ortiz, J. Cioslowski, D.J. Fox, GAUSSIAN 09, Revision A.1, Gaussian, Inc., Wallingford, CT, 2009.
- [36] S. Grimme, J. Antony, S. Ehrlich, H. Krieg, A consistent and accurate ab initio parametrization of density functional dispersion correction (DFT-D) for the 94 elements H – Pu, *J. Chem. Phys.* 132 (2010) 154104.
- [37] T.H. Dunning Jr., Gaussian basis sets for use in correlation molecular calculations. I. The atoms boron through neon and hydrogen, *J. Chem. Phys.* 90 (1989) 1007.
- [38] G. Cooke, J.F. Garety, B. Jordan, N. Kryvokhyzha, A. Parkin, G. Rabani, V.M. Rotello, Favin-based [2]rotaxanes, *Org. Lett.* 8 (2006) 2297–2300.
- [39] S. Cosnier, A. Karyakin, *Electropolymerization: Concepts, Materials and Applications*, Wiley-VCH Verlag, Weinheim, Germany, 2010.
- [40] N. Atilgan, A. Cihaner, A.M. Onal, Electrochromic performance and ion sensitivity of a terthienyl based fluorescent polymer, *React. Funct. Polym.* 70 (2010) 244–250.
- [41] J. Xu, Z. Wei, Y. Du, W. Zhou, S. Pu, Low-potential electrochemical polymerization of fluorene and its alkyl-polymer precursor, *Electrochim. Acta* 51 (2006) 4771–4779.
- [42] B. Bezgin, A. Cihaner, A.M. Önal, Electrochemical polymerization of 9-fluorene carboxylic acid and its electrochromic device application, *Thin Solid Films* 516 (2008) 7329–7334.
- [43] E. Sefer, H. Bilgili, B. Gultekin, M. Tonga, S. Koyuncu, A narrow range multi-electrochromism from 2,5-di-(2-thienyl)-1H-pyrrole polymer bearing pendant perylenediamine moiety, *Dyes Pigm.* 113 (2015) 121–128.
- [44] J. Roncali, Conjugated poly(thiophenes): synthesis, functionalization, and applications, *Chem. Rev.* 92 (1992) 711–738.
- [45] A.S. Ribeiro, L.M.O. Ribeiro, J.G. Silva Jr., M. Navarro, J. Tonholo, Characterization by atomic force microscopy of electrodeposited films of polypyrrole-dinitrobenzoyl derivative, *Microsc. Microanal.* 11 (2005) 146–149.
- [46] T. Soganci, S. Soyleyici, H.C. Soyleyici, M. Ak, Optoelectronic characterization and smart windows application of bi-functional amid substituted thietyl pyrrole derivative, *Polymer* 118 (2017) 40–48.
- [47] G. Nie, L. Qu, J. Xu, S. Zhang, Electrosyntheses and characterizations of a new soluble conducting copolymer of 5-cyanoindole and 3,4-ethylenedioxythiophene, *Electrochim. Acta* 53 (2008) 8351–8358.
- [48] G. Inzelt, M. Pineri, J.W. Schutze, M.A. Vorontsev, Electron and proton conducting polymers: recent developments and prospects, *Electrochim. Acta* 45 (2000) 2403–2421.
- [49] J.F. Rusling, S.L. Suib, Characterizing materials with cyclic voltammetry, *Adv. Mater.* 6 (1994) 922–930.
- [50] P.M. Beaujuge, J.R. Reynolds, Color control in  $\pi$ -conjugated organic polymers for use in electrochromic devices, *Chem. Rev.* 110 (2010) 268–320.
- [51] P. Camurlu, Polypyrrrole derivatives for electrochromic applications, *RSC Adv.* 4 (2014) 55832–55845.
- [52] N. Guven, P. Camurlu, Optoelectronic properties of poly(2,5-dithienylpyrrole)s with fluorophore groups, *J. Electrochem. Soc.* 162 (2015) H867–H876.
- [53] T. Soganci, H.C. Soyleyici, M. Ak, A soluble and fluorescent new type thietylpyrrole based conjugated polymer: optical, electrical and electrochemical properties, *Phys. Chem. Chem. Phys.* 18 (2016) 14401–14407.
- [54] A.J. Bard, L.R. Faulkner, *Electrochemical Methods, Fundamentals and Application*, John Wiley & Sons, New York, 1980.
- [55] L.B. Groenendaal, G. Zotti, P.H. Aubert, S.M. Waybright, J.R. Reynolds, Electrochemistry of poly(3,4-alkylenedioxythiophene) derivatives, *Adv. Mater.* 15 (11) (2003) 855–879.
- [56] M. Sato, S. Tanaka, K. Kaeriyama, Electrochemical preparation of conducting poly(3-methylthiophene): comparison with polythiophene and poly(3-ethylthiophene), *Synth. Met.* 14 (1986) 279–288.
- [57] T.C. Chung, J.H. Kaufman, A.J. Heeger, F. Wudl, Charge storage in doped poly(thiophene): Optical and electrochemical studies, *Phys. Rev. B* 30 (1984) 702–710.
- [58] T. Soganci, S. Soyleyici, H.C. Soyleyici, M. Ak, High contrast electrochromic polymer and copolymer materials based on amide-substituted poly(dithienylpyrrole), *J. Electrochem. Soc.* 164 (2017) H11–H20.
- [59] L.M.O. Ribeiro, J.Z. Auad, J.G. Silva Júnior, M. Navarro, A. Mirapalheta, C. Fonseca, S. Neves, J. Tonholo, A.S. Ribeiro, The effect of the conditions of electrodeposition on the capacitive properties of dinitrobenzoyl-derivative polypyrrrole films, *J. Power Sources* 177 (2008) 669–675.
- [60] S.P. Mucur, R. Kacar, C. Meric, S. Koyuncu, Thermal annealing effect on light emission profile of polyfluorines containing double bond subunit, *Org. Electron.* 50 (2017) 55–62.
- [61] Z.R. Grabowski, K. Rotkiewicz, W. Rettig, Structural changes accompanying intramolecular electron transfer: focus on twisted intramolecular charge-transfer states and structures, *Chem. Rev.* 103 (2003) 3899–4032.
- [62] T. Hayashi, N. Malaga, Y. Sakata, S. Misumi, M. Morita, J. Tanaka, Excimer fluorescence and photodimerization of anthracenophanes and 1,2-dianthrylethanes, *J. Am. Chem. Soc.* 98 (1976) 5910–5913.
- [63] W.T. Yip, D.H. Levy, Excimer/exciplex formation in van der Waals dimers of aromatic molecules, *J. Phys. Chem.* 100 (1996) 11539–11545.
- [64] H. Bouas-Laurent, A. Castellan, J.P. Desvergne, R. Lapouyade, Photodimerization of anthracenes in fluid solutions: (part 2) mechanistic aspects of the photo-cycloaddition and of the photochemical and thermal cleavage, *Chem. Soc. Rev.* 30 (2001) 248–263.